Influence of spin-phonon coupling on antiferromagnetic spin fluctuations in FeSe under pressure: First-principles calculations with van der Waals corrections

Qian-Qian Ye,[1] Kai Liu,[1,2,*] and Zhong-Yi Lu[1,2,†]

[1]*Department of Physics, Renmin University of China, Beijing 100872, China*

[2]*Beijing Key Laboratory of Opto-electronic Functional Materials & Micro-nano Devices, Beijing 100872, China*

(Received 13 October 2013; revised manuscript received 6 November 2013; published 21 November 2013)

The electronic structures, lattice dynamics, and magnetic properties of crystal β-FeSe under hydrostatic pressure have been studied by using the first-principles electronic structure calculations with van der Waals corrections. With applied pressure, the energy bands around the Fermi energy level consisting mainly of Fe-3*d* orbitals show obvious energy shifts and occupation variations, and meanwhile the frequencies of all optical phonon modes increase. Among these phonon modes, the A_{1g} mode, which relates to the Se height from the Fe-Fe plane, shows a clear frequency jump in a pressure range between 5 and 6 GPa. This is also the pressure range within which the highest superconducting transition temperature T_c of FeSe is reached in experiments. In comparison with other phonon modes, the atomic displacement due to the zero-point vibration of the A_{1g} mode induces the strongest fluctuation of local magnetic moment on Fe under pressures from 0 to 9 GPa, and the induced fluctuation reaches a maximum around 5 GPa. These results suggest that the effect of phonon via spin-phonon coupling could not be completely omitted when exploring the superconducting mechanism in iron-based superconductors.

DOI: 10.1103/PhysRevB.88.205130 PACS number(s): 74.70.Xa, 74.25.−q, 71.15.Mb, 63.20.kk

I. INTRODUCTION

With the simplest crystal structure among the iron-based superconductors ever found,[1–4] PbO-type β-FeSe has attracted tremendous attention both experimentally and theoretically as an archetype system to explore the unconventional superconductivity mechanism in the iron-based superconductors. The superconducting transition temperature T_c of FeSe is found to be 8 K at ambient pressure,[4] and is extremely sensitive to external pressures,[5] while it can grow to a maximum of ∼37 K around 6–9 GPa.[6–8] On the other hand, the nuclear magnetic resonance (NMR) measurement has found strongly enhanced antiferromagnetic (AFM) spin fluctuations near T_c and that both T_c and spin fluctuations are raised by pressures, suggesting a close correlation between the spin fluctuations and the superconducting mechanism in iron-based superconductors.[9]

With applied pressure, the crystal structure of β-FeSe encounters notable changes.[6–8] Its volume undergoes as high as 20% reduction and the interlayer spacing shows large decrease.[6,7] In contrast, the height of Se from the Fe-Fe plane first decreases and then increases with pressure.[7] By summarizing the T_cs of FeSe under pressures and the T_cs of various iron (and nickel)-based superconductors, a striking correlation between the T_c and the height of anion (i.e., Se in FeSe) is revealed.[8,10] Moreover, Moon and Choi found that the magnetic interactions and magnetic order are very sensitive to the height of chalcogen species from the Fe-Fe plane by studying the FeTe system with several fixed heights Z_{Te} by using the density-functional-theory (DFT) calculations.[11] It was also found that the height of chalcogen atoms above the Fe-Fe plane, rather than the chalcogen species or disorder, affects the magnetism and shape of Fermi surfaces of $FeTe_xSe_{1-x}$.[12] This is also reflected in the experiments that the nonsuperconducting FeTe bulk samples become superconducting in the FeTe thin films under tensile stress.[13] These observations indicate that the crystal structures and magnetic properties, both of which link with T_c in iron chalcogenide superconductors, are obviously correlated and can be tuned by an applied pressure.

A direct consequence of substantial changes in the crystal structure under pressure is that the lattice dynamics would be influenced. However, within the standard McMillan-Eliashberg framework, the electron-phonon coupling calculations without spin polarization give too low values for the transition temperature T_c of FeSe.[14] When the spin polarization effects are included, the calculated electron-phonon coupling value in the checkerboard AFM Néel order shows about a twofold increase, but still cannot account for the experimentally observed T_c of FeSe.[15] It is now commonly accepted that FeSe is not a conventional electron-phonon superconductor,[14] but a spin-fluctuation mediated unconventional superconductor.[16,17] Nevertheless, a clear iron isotope effect on T_c of FeSe has been observed in experiments,[18] and the magnetic properties have been found to be very sensitive to the lattice parameters of $FeSe_xTe_{1-x}$ from the DFT calculations,[11] thus we are curious about what role the lattice vibrations play in the spin fluctuations (via the spin-phonon coupling effect) of FeSe. More importantly, how the role of the lattice vibrations will change along with pressure, especially around the pressure with the highest T_c of FeSe, has never been studied.

As FeSe has Se-Fe_2-Se layers composed of edge-sharing tetrahedra with an Fe center, the van der Waals (vdW) interaction plays an important role in the interlayer bonding. When a pressure is applied, the interlayer distance of FeSe shows much larger reduction compared with the in-plane lattice constants.[6] In order to precisely describe the lattice dynamics of FeSe under pressure in calculations, the vdW interactions between FeSe layers need to be accurately accounted for. Since the conventional density functionals are unable to describe correctly the vdW interactions, which arise from nonlocal long-range electron correlations,[19,20] both nonlocal correlation functional[21–24] and a semiempirical dispersion potential[25,26] method have been proposed to include

the dispersion interactions. Nowadays, the DFT problem for vdW interaction has become a very active field and theoretical studies have been carried out on various molecules and materials.[20,26–32] However, the DFT calculations with vdW-interaction corrections have rarely been applied to the iron-based superconductors.[33,34]

We have studied the electronic structures, lattice dynamics, and magnetic properties of FeSe under pressure by using DFT calculations with vdW corrections. Especially, the variations of the band structures and phonon frequencies from 0 to 9 GPa, as well as the effect of zero-point vibrations of phonon modes on the local magnetic moment fluctuations and the band structures, have been addressed.

II. COMPUTATIONAL DETAILS

The first-principles electronic structure calculations were carried out with the Vienna *ab initio* simulation package,[35,36] which makes use of the projector augmented wave (PAW) method.[37] The exchange-correlation functionals were represented by the generalized gradient approximation (GGA) of Perdew-Burke-Ernzerhof (PBE) type.[38] In order to describe the vdW interactions not included in the conventional density functional, our calculations adopted the DFT-D2 method[25,26] with semiempirical dispersion energy adding to the Kohn-Sham DFT energy. The energy cutoff for the plane waves was set to 350 eV. The $1 \times 1 \times 1$ tetragonal cell of FeSe was used and the integration over the Brillouin zone was performed with a $12 \times 12 \times 12$ **k**-point mesh. The Fermi level was broadened by the Gaussian smearing method with a width of 0.05 eV. Both cell parameters and internal atomic positions were allowed to relax. The system under hydrostatic pressures in a range of 0 to 9 GPa was simulated by assigning the converged trace of stress tensor to a targeting pressure and minimizing the enthalpy of the system. In the studied pressure range, the structure of FeSe has not changed to hexagonal.[6] The atoms were allowed to relax until the forces were smaller than 0.01 eV/Å. After the equilibrium structures were obtained, the frequencies and displacement patterns of the phonon modes were calculated by using the dynamical matrix method.[39] The atomic displacements due to the zero-point vibrations of the phonon modes were obtained according to the method of Ref. 40. In the present case, the atoms were displaced to the vibrational state with a potential energy of $\hbar\omega_s/2$ for a specified phonon mode s, while its normal-mode coordinates can reach two maxima along two opposite directions.

There is another issue in the calculations that needs to be addressed, i.e., the magnetic order that we choose in this study. From first-principles calculations, the magnetic ground states of most iron-based superconductors at low temperature are in the stripe collinear AFM order. But unlike other iron pnictides such as LaOFeAs[41] and $BaFe_2As_2$,[42] no long-range magnetic order has been found for β-FeSe at ambient pressure in experiment. This may be related to the fact that the samples of β-FeSe with a strict ratio of 1:1 have not been synthesized in experiment and the content of Fe is always a little extra. However, the strong AFM spin fluctuations have been observed for the undoped FeSe.[9] Theoretically, it is very difficult to directly simulate such a paramagnetic phase by using DFT calculations. Considering that the checkerboard-AFM Néel order and the paramagnetic phase share the following important features, (1) local moments around Fe atoms, (2) zero net magnetic moment in a unit cell, and (3) the same space symmetry, the checkerboard-AFM Néel state can be thus feasible to properly model the paramagnetic phase in many aspects.[15,43] Especially, for the recently grown FeSe monolayer on $SrTiO_3$ with signatures of T_c above 50 K by transport measurement,[44] the observed shape of Fermi surface in angle-resolved photoemission spectroscopy (ARPES) experiments[45–47] can be reproduced in the DFT calculations by the AFM Néel order of FeSe monolayer either without substrate[48] or on $SrTiO_3$ surface.[49] In Table I, our calculated lattice parameters for bulk FeSe in nonmagnetic and AFM Néel states with or without vdW interactions are compared with the experimental results. As listed in the table, the calculated structure parameters in the AFM Néel order with vdW interaction show the best overall agreement with the experimental ones[50,51] and also yield the better results than the previous calculations by using PBE and hybrid functionals.[52] More importantly, the lattice constant along the stacking direction which changes most under pressure is well reproduced. In recent muon-spin rotation and relaxation (μSR) and magnetization experiments, the antiferromagnetism of FeSe has been found to occur under a pressure around 1.0 GPa and coexist microscopically with superconductivity.[53] So we choose the AFM Néel order to simulate the FeSe under pressure in the following studies.

TABLE I. Calculated fully relaxed lattice parameters for bulk FeSe in nonmagnetic and AFM Néel states with or without vdW interactions along with the experimental results.

	a (Å)	b (Å)	c (Å)	Z_{Se} (Å)
NM				
No-vdW	3.679	3.679	5.999	1.385
vdW	3.632	3.632	5.382	1.397
Néel				
No-vdW	3.710	3.710	6.305	1.437
vdW	3.654	3.654	5.471	1.436
Expt. (7 K)[50]	3.765	3.754	5.479	1.462
Expt. (298 K)[51]	3.773	3.773	5.526	1.476

Regarding the vdW correction to the conventional DFT functionals, the more accurate vdW-optB86b functional,[27] which includes the nonlocal vdW interaction in the exchange and correlation functionals, was also adopted in the studies of FeSe at ambient pressure in order to examine the influence of different vdW approaches. Consistent results of the vdW-optB86b functional and the DFT-D2 method were obtained for the lattice parameters and the interlayer bonding energy ($\sim$26 meV/Å^2). These are in accordance with the previous calculations.[29,33,34]

III. RESULTS AND ANALYSIS

Applying pressure on bulk FeSe can result in dramatic changes in its electronic band structure. The energy band near the Fermi level at Γ point (labeled by orange line) is occupied at zero pressure [Fig. 1(a)] and becomes unoccupied at 5 and 6 GPa [Figs. 1(b) and 1(c)]. Based on the analysis of band-decomposed charge density, it is confirmed that this

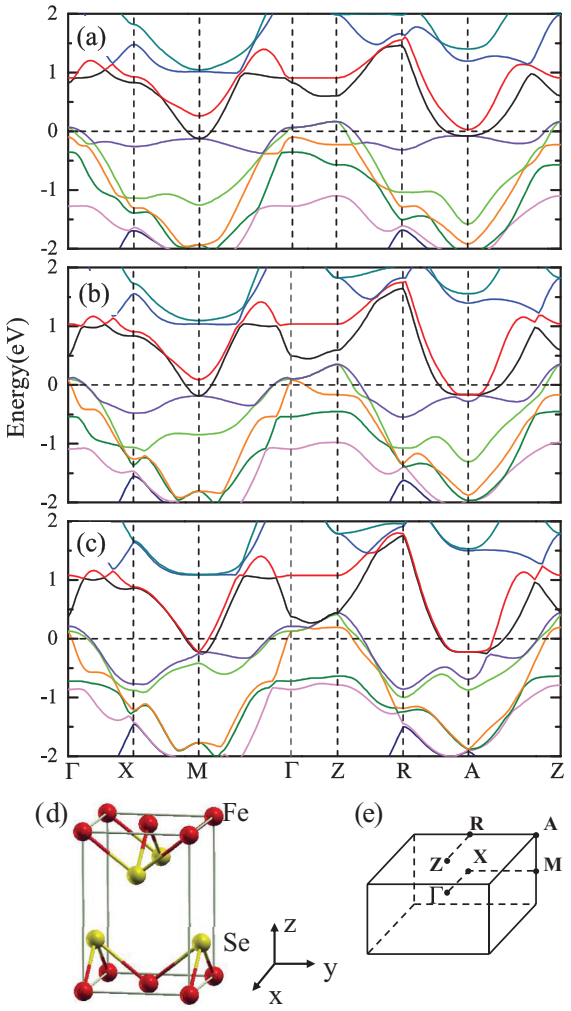

FIG. 1. (Color online) Electronic band structures of FeSe in the checkerboard AFM Néel state under a pressure of (a) 0, (b) 5, and (c) 6 GPa. The Fermi energy is set to zero. Panels (d) and (e) are the tetragonal cell and the corresponding Brillouin zone, respectively.

band consists of the $d_{x^2-y^2}$ orbital of Fe at 0 and 5 GPa and changes into the d_{xz}/d_{yz} orbitals at 6 GPa. Around M point, the unoccupied energy band near the Fermi level (in red color) at 0 and 5 GPa becomes occupied at 6 GPa. After the same analysis on charge density, it is ascertained that this band originates from the $d_{x^2-y^2}$ orbital of Fe at 0 and 5 Gpa and becomes the d_{xz}/d_{yz} orbitals at 6 GPa. The hole pockets around Γ point and the electron pockets around M point are consistent with the previous ARPES experimental measurement.[54] In addition to the Γ and M points, the band structures also show obvious changes around Z and A points, which are similar to those around Γ and M points. Thus the occupations of the energy bands around the Fermi level which originate mainly from the d_{xz}/d_{yz} and $d_{x^2-y^2}$ orbitals of Fe are very sensitive to pressure. From the analysis on the calculated density of states, the contribution around the Fermi level from Se atom is minor. These calculation results are in accord with a recent study combining ARPES experiment and DFT calculations on $FeTe_{0.66}Se_{0.34}$.[55] In our calculations, the applied pressure makes the crystal lattice constants of FeSe decrease, especially

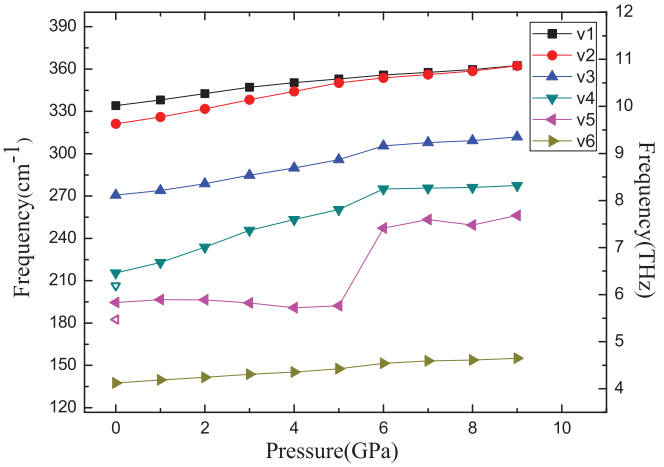

FIG. 2. (Color online) Calculated phonon frequencies at Brillouin zone center for FeSe in the checkerboard AFM Néel order under pressures from 0 to 9 GPa. Hollow triangles at 0 GPa label the corresponding experimental data from Raman scattering measurements.[56] Phonon modes v1, v2, v3, v4, v5, and v6 here are schematically shown in Fig. 3, respectively.

resulting in the collapse of separation between FeSe layers from 5.47 Å at 0 GPa to 4.99 Å at 6 GPa. This will lead to corresponding changes in the electronic properties such as the band structures and orbital occupations.

Not only the electronic band structures show large changes with pressure, but also the lattice dynamics demonstrates obvious variations. As shown in Fig. 2, the frequencies of all optical phonon modes of FeSe at Brillouin zone center increase with pressure. These modes are labeled in the sequence of energy. Among these phonon modes, the frequency of mode v5 has a clear sharp jump from 5 to 6 GPa. The hollow triangles represent the experimental results of Raman scattering,[56] which are in the same color as the corresponding calculated values. By comparison between experiment and calculation, there is only about 5% deviation for the frequencies of modes v4 and v5. This ascertains our theoretical approach by using the checkerboard AFM Néel state. In contrast, the frequencies calculated by using fully relaxed structure in nonmagnetic state with vdW interaction show much worse agreement (∼30% deviation) with experiment. And the phonon frequencies in nonmagnetic state increase slowly with pressure and show just about 1–3 meV energy change from 0 to 9 GPa. In a recent Raman-scattering measurement on $K_{0.8}Fe_{1.6}Se_2$, an anomalous hardening was observed for the A_g mode around T_c, indicating a particular type of connection between phonons and superconductivity.[57] In our calculations, both the frequency (194.5 cm^{-1}) and the symmetry (A_{1g}, shown below) of mode v5 for FeSe are similar to the 180 cm^{-1} A_g mode in $K_{0.8}Fe_{1.6}Se_2$.[57] Some experiments on FeSe have shown that depending on a specific method to apply pressure, a maximum T_c of 37 K can be reached under pressures approximately 6–9 GPa.[6,7] The anomalous frequency jump of phonon mode v5 around the similar pressure range indicates some relationship between this mode and the superconductivity of FeSe.

In order to identify the characteristics of each phonon mode, we plot the atomic displacement patterns at 6 GPa in Fig. 3. The

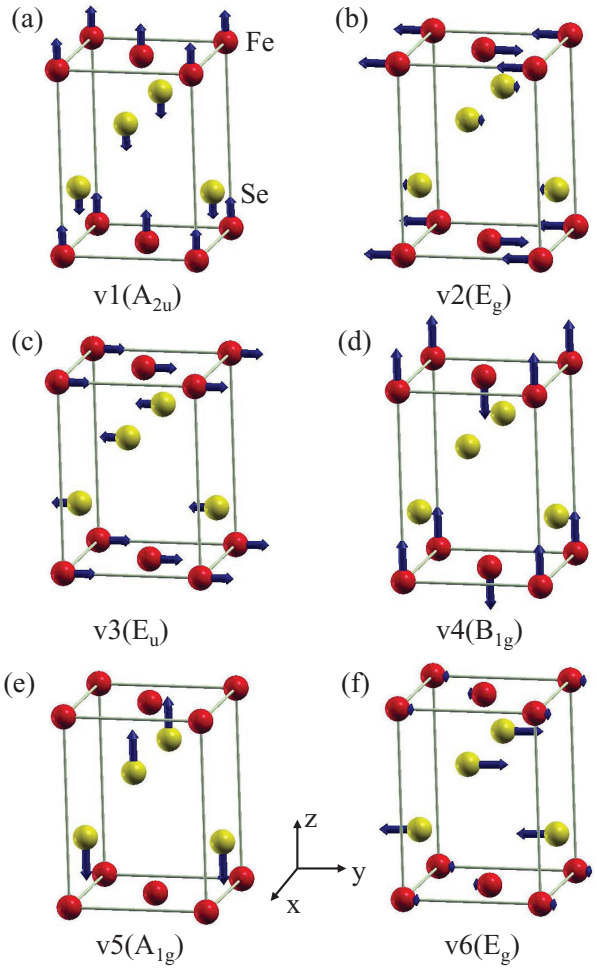

FIG. 3. (Color online) Atomic displacement patterns respectively for modes (a) v1 (A_{2u}), (b) v2 (E_g), (c) v3 (E_u), (d) v4 (B_{1g}), (e) v5 (A_{1g}), and (f) v6 (E_g) at 6 GPa pressure with corresponding symmetries in the parentheses.

displacement arrows are in the same scale among all panels. For mode v1, the atoms show the same displacement directions for the same atomic species and the opposite movements for different species. It is an infrared active A_{2u} mode. Modes v2, v3, and v6 are all doubly degenerate in-plane vibrations, while modes v2 and v6 are Raman active and mode v3 is infrared active. Both modes v4 and v5 are out-of-plane vibrations. Mode v4 consists of the opposite vertical motions of Fe atoms in the same Fe-Fe plane, while mode v5 involves the coherent motions of Se atoms relative to their adjacent Fe-Fe planes. The atomic displacement patterns are consistent with the previous studies.[58] In Ref. 8, the authors have found that the anion height relative to the Fe-Fe plane is a key factor to influence the T_c of iron-based superconductors. Among all phonon modes of FeSe, the atomic displacements in modes v1 and v5 change the Se height mostly. However, in mode v1, the Se atoms above and below the Fe-Fe plane show opposite height changes and break the original spatial symmetry of FeSe. Meanwhile, the displacements of Se atoms in the A_{1g} mode v5 control precisely the Se height from the Fe-Fe plane and keep the same symmetry as that before moving. In recent time- and angle-resolved photoemission experiments on $EuFe_2As_2$,[59]

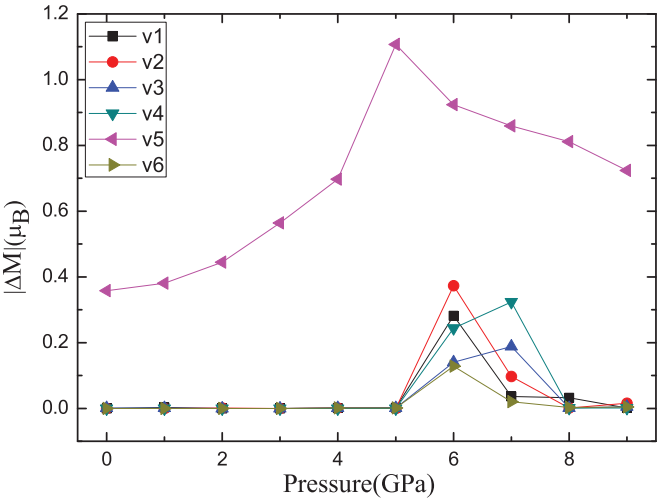

FIG. 4. (Color online) Changes of local magnetic moment fluctuations on Fe induced by the atomic displacements due to the zero-point vibrations of different optical phonon modes versus pressure.

the modulations of electron and hole dynamics due to the A_{1g} phonon have been observed. Using femtosecond optical pulses, Kim *et al.* have also detected the transient magnetic ordering in $BaFe_2As_2$ quasiadiabatically follows the lattice vibrations of an A_{1g} mode with a frequency of 5.5 THz.[60] Due to a sharp increase of the phonon frequency at 6 GPa for the A_{1g} mode v5 of FeSe (Fig. 2), it is very tempting to deduce that the A_{1g} phonon mode plays an important role in the T_c increase of FeSe under pressure.

Considering the substantial increase of phonon frequency with pressure, we simulate the atomic displacements due to the zero-point vibrations of all optical phonons in order to study their influence on the magnetic moments of FeSe under pressure. The FeSe system is set to the vibrational state with a zero-point energy of $\hbar\omega_s/2$ in each specified phonon mode s, in which the normal-mode coordinate could reach maxima along two opposite directions. So there are two displacement patterns for each mode at each pressure. We plot the difference of local magnetic moment on Fe between the two displacement patterns of each mode at various pressures (see Fig. 4), namely $|\triangle M| = |M_+ - M_-|$, with M_+ being the local magnetic moment on Fe for one displacement and M_- the other. From Fig. 4, we see that $|\triangle M|$ induced by the atomic displacement due to the zero-point vibration of mode v5 has much larger values than the corresponding ones for all other phonon modes in the whole pressure range, and it reaches the maximum value at 5 GPa. For the zero-point vibrations induced by the other phonon modes, $|\triangle M|$ are not zero only around 6 GPa. So it can be concluded that all the phonon modes enhance the AFM fluctuations around 6 GPa. This is in accordance with the experimental observations that the application of pressure on FeSe enhances the AFM spin fluctuations.[9] As the pressure increases, the occupations of the energy bands around the Fermi level, which consist of Fe 3d orbitals, show large variations (Fig. 1). The sensitive occupations of these Fe 3d orbitals to the lattice vibrations are responsible for the local magnetic moment fluctuations. In addition, the local magnetic moment M on Fe in FeSe at equilibrium structure gets smaller and smaller with increasing pressure. A similar

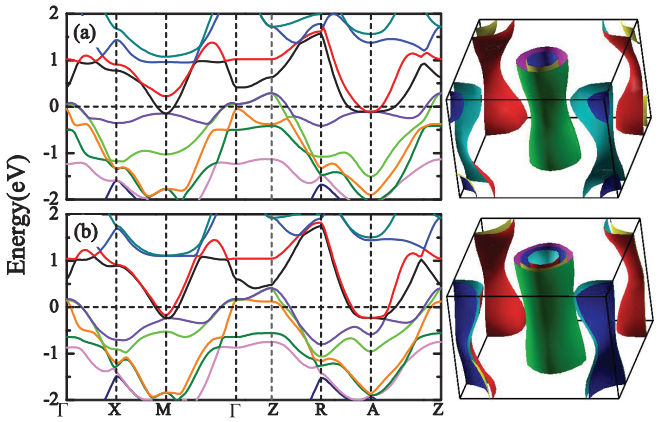

FIG. 5. (Color online) Electronic band structures and Fermi surfaces of FeSe in the checkerboard AFM Néel state as a result of the atomic displacement due to the zero-point vibration of the A_{1g} mode at 5 GPa. The Fermi energy is set to zero. Panels (a) and (b) correspond to movements of atom Se far away from and close to the Fe-Fe plane, respectively. The high symmetry points in Brillouin zone are the same as that in Fig. 1(e).

reduction tendency of the local magnetic moment on Fe with pressure has also been found in the stripe collinear AFM order, whose energy is lower than that of the checkerboard AFM Néel order by 31–38 meV per Fe atom, depending on the applied pressure. The reduction magnitudes of local magnetic moment are somewhat different, i.e., ∼0.3 μB in the collinear order vs ∼1.0 μB in the Néel order. This means that the pressure suppresses the AFM state. With the anomalous frequency increase of phonon mode v5 (Fig. 2) and the enhanced magnetic moment fluctuations by the lattice vibrations around 5–6 GPa (Fig. 4), we have shown that the spin-phonon coupling plays an important role in FeSe under pressure.

Although the atomic displacements due to the zero-point vibration of the A_{1g} mode are very small (about 0.03 Å), their impact on the electronic band structure is distinct. Figure 5 shows the corresponding band structures with the atomic displacements due to the zero-point vibration of the A_{1g} mode when Se moves (a) away from and (b) close to the Fe-Fe plane at 5 GPa. At Γ point, the band around the Fermi level labeled by the orange line is occupied when Se moves away from the Fe-Fe plane [Fig. 5(a)] and becomes unoccupied when Se moves close [Fig. 5(b)]. Through analysis on the band-decomposed charge density, this band consists of the Fe $d_{x^2-y^2}$ orbital in Fig. 5(a) and changes into the d_{xz}/d_{yz} orbital in Fig. 5(b). Around M point, the energy band represented by the red line shows the opposite change to that at Γ point. After the charge analysis, it is confirmed that this red color band around M point comes from the $d_{x^2-y^2}$ orbital of Fe. The energy bands around Z and A points, which show occupation changes with the atomic displacements due to the zero-point vibration of the A_{1g} mode, also involve the $d_{x^2-y^2}$ and d_{xz}/d_{yz} orbitals of Fe. Thus the atomic displacement due to the zero-point vibration of the A_{1g} mode induces electron scattering between different 3d orbitals of Fe atom. The three-dimensional views can be seen more clearly from the shape changes of Fermi surfaces as plotted adjacent to the corresponding band structures. Small changes of the crystal structure (∼0.03 Å) due to the atomic displacements under the zero-point vibrations of phonon modes alone could not affect the energy band so much unless some other physical mechanism is included in this process. Actually, nonmagnetic calculations have been performed, which ascertain this speculation. The atomic displacements due to the zero-point vibrations of frozen phonon modes have great impact on the energy bands only in spin-polarized calculations. The dramatic changes of band structures and Fermi surfaces due to the zero-point vibrations of A_{1g} mode further support that the spin-phonon coupling plays an important role in FeSe under pressure.

IV. DISCUSSION AND SUMMARY

Our above calculations show that the zero-point vibration of the A_{1g} mode of FeSe, which relates to the Se height from the Fe-Fe plane, induces large fluctuations of local magnetic moment on Fe via the spin-phonon coupling, and further enhances the fluctuations under pressure. In recent experiments by means of magnetization and neutron powder diffraction, a clear isotope effect on T_c is observed for bulk FeSe, which highlights the role of the lattice in the pairing mechanism.[18] In a Raman-scattering measurement on $K_{0.8}Fe_{1.6}Se_2$, an anomaly at T_c in the 180 cm^{-1} A_g mode is observed, which indicates a rather specific type of electron-phonon coupling.[57] For the recently grown FeSe monolayer on $SrTiO_3$, which shows T_c signature above 50 K,[44] the screening due to the $SrTiO_3$ ferroelectric phonons on Cooper pairing in monolayer FeSe is proposed to significantly enhance the energy scale of Cooper pairing and even change the pairing symmetry.[61] From the first-principles studies on FeSe and KFe_2Se_2, the estimates of T_c based on spin-resolved coupling values show around a twofold increase than that from non-spin-resolved configurations.[15] These experimental and theoretical studies all suggest that the effect of phonon could not be ignored in the pairing mechanism of FeSe.

Not only in iron chalcogenides, there are also evidences of phonon effects on the unconventional superconductivity in iron pnictides and cuprates. On the experimental side, for $SmFeAsO_{1-x}F_x$ and $Ba_{1-x}K_xFe_2As_2$ compounds, the iron isotope substitution shows the same effect on T_c and the spin-density-wave transition temperature T_{SDW}, suggesting that strong magnon-phonon coupling exists.[62] Using ultrashort and intense optical pulses probe, an ultrafast transient spin-density-wave order develops in the normal state of $BaFe_2As_2$ and is driven by coherent lattice vibrations even without breaking the crystal symmetry, which attests a pronounced spin-phonon coupling in pnictides.[60] From ARPES probing of the electron dynamics in three different families of copper oxide superconductors,[63] which share a common thread of spin-fluctuation mediated pairing as iron-based superconductors,[17] it was found that an abrupt change of electron velocity at 50–80 meV cannot be explained by any known process other than the coupling to phonon is included.[63] On the theoretical side, Yildirim found strong coupling of the on-site Fe-magnetic moment with the As-As bonding in iron-pnictide superconductors from the first-principles calculations.[64] For computational studies on doped LaFeAsO, the coupling magnetism with vibrations was also found to induce anharmonicities and electron-phonon interaction much

larger than in the paramagnetic state.[65,66] From these studies, we see that the effect of spin-phonon coupling is evidently ubiquitous in iron-based superconductors.

The spin-fluctuation mediated pairing is common in iron-based superconductors and other unconventional superconducting materials.[16,17] Regarding the nature of the magnetism in iron-based superconductors, there are basically two contradictive views. The one is based on the itinerant electron picture,[67] in which the Fermi surface nesting is responsible for the AFM order. On the contrary, the other one is based on local moment interactions which can be described by the J_1-J_2 frustrated Heisenberg model.[68–70] And it was further shown[70] that the underlying driving force herein is the anion-bridged AFM superexchange interaction between a pair of the next-nearest-neighboring fluctuating Fe local moments embedded in itinerant electrons. There is now more and more evidence in favor of the fluctuating Fe local moment picture. Especially, the inelastic neutron scattering experiments have shown that the low-energy magnetic excitations can be well described by the spin waves based on the J_1-J_2 Heisenberg model.[71,72] Our calculated results of FeSe here show that the phonon frequencies calculated with local magnetic moment on Fe show a better agreement with the experiments than those with the nonmagnetic state. The fluctuations of local magnetic moment induced by the atomic displacement due to the zero-point vibration of the A_{1g} phonon mode are significant and further enhanced under pressure. Even though the direct electron-phonon coupling calculations both without[14] and with[15] spin polarization effects cannot account for the experimentally observed T_c of FeSe, the phonon may play an important role through spin-phonon coupling. Our results show that the effect of spin-phonon coupling could not be completely ignored when unraveling the pairing mechanism in iron-based superconductors.

To summarize, the variation of band structures and phonon frequencies of FeSe under 0 to 9 GPa hydrostatic pressure, as well as the effect of the atomic displacements due to the zero-point vibrations on the local magnetic moment fluctuations and band structures, have been investigated by using DFT calculations with vdW corrections. With applied pressure, the energy bands consisting of Fe 3d orbitals around the Fermi level show obvious shifts and occupation changes. At the same time, the frequencies of all optical phonon modes at Brillouin zone center increase with pressure. Among these phonon modes, the A_{1g} mode related to the Se height from an Fe-Fe plane shows a clear frequency jump from 5 to 6 GPa. This is around the similar pressure range within which the highest T_c is observed for FeSe in experiment. Compared with the other phonon modes, the atomic displacement due to the zero-point vibration of the A_{1g} mode also induces the strongest fluctuation of local magnetic moment on Fe from 0 to 9 GPa and the fluctuation reaches the maximum at 5 GPa. The enhanced fluctuations of local magnetic moment may be favorable to promote the T_c. These results suggest that the spin-phonon coupling may have an important impact on the iron-based superconductors.

ACKNOWLEDGMENTS

We wish to thank Professor Shiwu Gao for helpful communications. This work is supported by National Natural Science Foundation of China (Grants No. 11004243, No. 11190024, and No. 51271197) and National Program for Basic Research of MOST of China (Grant No. 2011CBA00112). Computational resources have been provided by the Physical Laboratory of High Performance Computing at Renmin University of China. The atomic structures and Fermi surfaces were prepared with the XCRYSDEN program.[73]

*kliu@ruc.edu.cn
†zlu@ruc.edu.cn

[1] Y. Kamihara, T. Watanabe, M. Hirano, and H. Hosono, J. Am. Chem. Soc. **130**, 3296 (2008); X. H. Chen, T. Wu, G. Wu, R. H. Liu, H. Chen, and D. F. Fang, Nature (London) **453**, 761 (2008); G. F. Chen, Z. Li, D. Wu, G. Li, W. Z. Hu, J. Dong, P. Zheng, J. L. Luo, and N. L. Wang, Phys. Rev. Lett. **100**, 247002 (2008).
[2] M. Rotter, M. Tegel, and D. Johrendt, Phys. Rev. Lett. **101**, 107006 (2008).
[3] X. C. Wang, Q. Q. Liu, Y. X. Lv, W. B. Gao, L. X. Yang, R. C. Yu, F. Y. Li, and C. Q. Jin, Solid State Commun. **148**, 538 (2008).
[4] F. C. Hsu, J. Y. Luo, K. W. Yeh, T. K. Chen, T. W. Huang, P. M. Wu, Y. C. Lee, Y. L. Huang, Y. Y. Chu, D. C. Yan, and M. K. Wu, Proc. Natl. Acad. Sci. USA **105**, 14262 (2008).
[5] Y. Mizuguchi, F. Tomioka, S. Tsuda, T. Yamaguchi, and Y. Takano, Appl. Phys. Lett. **93**, 152505 (2008).
[6] S. Medvedev, T. M. McQueen, I. A. Troyan, T. Palasyuk, M. I. Eremets, R. J. Cava, S. Naghavi, F. Casper, V. Ksenofontov, G. Wortmann, and C. Felser, Nat. Mater. **8**, 630 (2009).
[7] S. Margadonna, Y. Takabayashi, Y. Ohishi, Y. Mizuguchi, Y. Takano, T. Kagayama, T. Nakagawa, M. Takata, and K. Prassides, Phys. Rev. B **80**, 064506 (2009).
[8] H. Okabe, N. Takeshita, K. Horigane, T. Muranaka, and J. Akimitsu, Phys. Rev. B **81**, 205119 (2010).
[9] T. Imai, K. Ahilan, F. L. Ning, T. M. McQueen, and R. J. Cava, Phys. Rev. Lett. **102**, 177005 (2009).
[10] Y. Mizuguchi, Y. Hara, K. Deguchi, S. Tsuda, T. Yamaguchi, K. Takeda, H. Kotegawa, H. Tou, and Y. Takano, Supercond. Sci. Technol. **23**, 054013 (2010).
[11] C. Y. Moon and H. J. Choi, Phys. Rev. Lett. **104**, 057003 (2010).
[12] J. Kumar, S. Auluck, P. K. Ahluwalia, and V. P. S. Awana, Supercond. Sci. Technol. **25**, 095002 (2012).
[13] Y. Han, W. Y. Li, L. X. Cao, X. Y. Wang, B. Xu, B. R. Zhao, Y. Q. Guo, and J. L. Yang, Phys. Rev. Lett. **104**, 017003 (2010).
[14] A. Subedi, L. Zhang, D. J. Singh, and M. H. Du, Phys. Rev. B **78**, 134514 (2008).
[15] T. Bazhirov and M. L. Cohen, Phys. Rev. B **86**, 134517 (2012).
[16] G. R. Stewart, Rev. Mod. Phys. **83**, 1589 (2011).
[17] D. J. Scalapino, Rev. Mod. Phys. **84**, 1383 (2012).
[18] R. Khasanov, M. Bendele, K. Conder, H. Keller, E. Pomjakushina, and V. Pomjakushin, New J. Phys. **12**, 073024 (2010).
[19] Y. Andersson, D. C. Langreth, and B. I. Lundqvist, Phys. Rev. Lett. **76**, 102 (1996).

[20]D. C. Langreth, B. I. Lundqvist, S. D. Chakarova-Käck, V. R. Cooper, M. Dion, P. Hyldgaard, A. Kelkkanen, J. Kleis, L. Z. Kong, S. Li, P. G. Moses, E. Murray, A. Puzder, H. Rydberg, E. Schröder, and T. Thonhauser, J. Phys.: Condens. Matter **21**, 084203 (2009).
[21]M. Dion, H. Rydberg, E. Schröder, D. C. Langreth, and B. I. Lundqvist, Phys. Rev. Lett. **92**, 246401 (2004); **95**, 109902 (2005).
[22]G. Román-Pérez and J. M. Soler, Phys. Rev. Lett. **103**, 096102 (2009).
[23]J. Klimeš, D. R. Bowler, and A. Michaelides, J. Phys.: Condens. Matter **22**, 022201 (2010).
[24]K. Lee, É. D. Murray, L. Kong, B. I. Lundqvist, and D. C. Langreth, Phys. Rev. B **82**, 081101 (2010).
[25]X. Wu, M. C. Vargas, S. Nayak, V. Lotrich, and G. Scoles, J. Chem. Phys. **115**, 8748 (2001).
[26]S. Grimme, J. Comput. Chem. **27**, 1787 (2006).
[27]J. Klimeš, D. R. Bowler, and A. Michaelides, Phys. Rev. B **83**, 195131 (2011).
[28]B. Santra, J. Klimeš, D. Alfè, A. Tkatchenko, B. Slater, A. Michaelides, R. Car, and M. Scheffler, Phys. Rev. Lett. **107**, 185701 (2011).
[29]T. Björkman, A. Gulans, A. V. Krasheninnikov, and R. M. Nieminen, Phys. Rev. Lett. **108**, 235502 (2012).
[30]S. V. Aradhya, M. Frei, M. S. Hybertsen, and L. Venkataraman, Nat. Mater. **11**, 872 (2012).
[31]K. Berland and P. Hyldgaard, Phys. Rev. B **87**, 205421 (2013).
[32]J. Phys.: Condens. Matter **24**(42) (2012), Special issue on van der Waals interactions in advanced materials, http://m.iopscience.iop.org/0953-8984/24/42.
[33]F. Ricci and G. Profeta, Phys. Rev. B **87**, 184105 (2013).
[34]H. Nakamura and M. Machida, Physica C **494**, 9 (2013).
[35]G. Kresse and J. Hafner, Phys. Rev. B **47**, 558 (1993); J. Phys.: Condens. Matter **6**, 8245 (1994).
[36]G. Kresse and J. Furthmüller, Comput. Mater. Sci. **6**, 15 (1996); Phys. Rev. B **54**, 11169 (1996).
[37]P. E. Blöchl, Phys. Rev. B **50**, 17953 (1994); G. Kresse and D. Joubert, *ibid*. **59**, 1758 (1999).
[38]J. P. Perdew, K. Burke, and M. Ernzerhof, Phys. Rev. Lett. **77**, 3865 (1996).
[39]K. Liu and S. Gao, Phys. Rev. Lett. **95**, 226102 (2005).
[40]D. West and S. K. Estreicher, Phys. Rev. Lett. **96**, 115504 (2006).
[41]C. de la Cruz, Q. Huang, J. W. Lynn, J. Li, W. Ratcliff, II, J. L. Zarestky, H. A. Mook, G. F. Chen, J. L. Luo, N. L. Wang, and P. C. Dai, Nature (London) **453**, 899 (2008).
[42]M. Rotter, M. Tegel, D. Johrendt, I. Schellenberg, W. Hermes, and R. Pöttgen, Phys. Rev. B **78**, 020503(R) (2008).
[43]W. Ji, X. W. Yan, and Z. Y. Lu, Phys. Rev. B **83**, 132504 (2011).
[44]Q.-Y. Wang, Z. Li, W.-H. Zhang, Z.-C. Zhang, J.-S. Zhang, W. Li, H. Ding, Y.-B. Ou, P. Deng, K. Chang, J. Wen, C.-L. Song, K. He, J.-F. Jia, S.-H. Ji, Y.-Y. Wang, L.-L. Wang, X. Chen, X.-C. Ma, and Q.-K. Xue, Chin. Phys. Lett. **29**, 037402 (2012).
[45]D. F. Liu, W. H. Zhang, D. X. Mou, J. F. He, Y.-B. Ou, Q.-Y. Wang, Z. Li, L. L. Wang, L. Zhao, S. L. He, Y. Y. Peng, X. Liu, C. Y. Chen, L. Yu, G. D. Liu, X. L. Dong, J. Zhang, C. T. Chen, Z. Y. Xu, J. P. Hu, X. Chen, X. C. Ma, Q. K. Xue, and X. J. Zhou, Nat. Commun. **3**, 931 (2012).
[46]S. L. He, J. F. He, W. H. Zhang, L. Zhao, D. F. Liu, X. Liu, D. X. Mou, Y. B. Ou, Q. Y. Wang, Z. Li, L. L. Wang, Y. Y. Peng, Y. Liu, C. Y. Chen, L. Yu, G. D. Liu, X. L. Dong, J. Zhang, C. T. Chen, Z. Y. Xu, X. Chen, X. C. Ma, Q. K. Xue, and X. J. Zhou, Nat. Mater. **12**, 605 (2013).
[47]S. Y. Tan, Y. Zhang, M. Xia, Z. R. Ye, F. Chen, X. Xie, R. Peng, D. F. Xu, Q. Fan, H. C. Xu, J. Jiang, T. Zhang, X. C. Lai, T. Xiang, J. P. Hu, B. P. Xie, and D. L. Feng, Nat. Mater. **12**, 634 (2013).
[48]T. Bazhirov and M. L. Cohen, J. Phys.: Condens. Matter **25**, 105506 (2013).
[49]F. W. Zheng, Z. G. Wang, W. Kang, and P. Zhang, Sci. Rep. **3**, 2213 (2013).
[50]D. Louca, K. Horigane, A. Llobet, R. Arita, S. Ji, N. Katayama, S. Konbu, K. Nakamura, T.-Y. Koo, P. Tong, and K. Yamada, Phys. Rev. B **81**, 134524 (2010).
[51]T. M. McQueen, Q. Huang, V. Ksenofontov, C. Felser, Q. Xu, H. Zandbergen, Y. S. Hor, J. Allred, A. J. Williams, D. Qu, J. Checkelsky, N. P. Ong, and R. J. Cava, Phys. Rev. B **79**, 014522 (2009).
[52]K. Liu and Z.-Y. Lu, Comput. Mater. Sci. **55**, 284 (2012).
[53]M. Bendele, A. Amato, K. Conder, M. Elender, H. Keller, H.-H. Klauss, H. Luetkens, E. Pomjakushina, A. Raselli, and R. Khasanov, Phys. Rev. Lett. **104**, 087003 (2010).
[54]A. Tamai, A. Y. Ganin, E. Rozbicki, J. Bacsa, W. Meevasana, P. D. C. King, M. Caffio, R. Schaub, S. Margadonna, K. Prassides, M. J. Rosseinsky, and F. Baumberger, Phys. Rev. Lett. **104**, 097002 (2010).
[55]F. Chen, B. Zhou, Y. Zhang, J. Wei, H.-W. Ou, J.-F. Zhao, C. He, Q.-Q. Ge, M. Arita, K. Shimada, H. Namatame, M. Taniguchi, Z.-Y. Lu, J. P. Hu, X.-Y. Cui, and D. L. Feng, Phys. Rev. B **81**, 014526 (2010).
[56]V. Gnezdilov, Y. G. Pashkevich, P. Lemmens, D. Wulferding, T. Shevtsova, A. Gusev, D. Chareev, and A. Vasiliev, Phys. Rev. B **87**, 144508 (2013).
[57]A. M. Zhang, K. Liu, J. H. Xiao, J. B. He, D. M. Wang, G. F. Chen, B. Normand, and Q. M. Zhang, Phys. Rev. B **85**, 024518 (2012).
[58]T.-L. Xia, D. Hou, S. C. Zhao, A. M. Zhang, G. F. Chen, J. L. Luo, N. L. Wang, J. H. Wei, Z.-Y. Lu, and Q. M. Zhang, Phys. Rev. B **79**, 140510(R) (2009).
[59]L. Rettig, R. Cortés, S. Thirupathaiah, P. Gegenwart, H. S. Jeevan, M. Wolf, J. Fink, and U. Bovensiepen, Phys. Rev. Lett. **108**, 097002 (2012).
[60]K. W. Kim, A. Pashkin, H. Schäfer, M. Beyer, M. Porer, T. Wolf, C. Bernhard, J. Demsar, R. Huber, and A. Leitenstorfer, Nat. Mater. **11**, 497 (2012).
[61]Y.-Y. Xiang, F. Wang, D. Wang, Q.-H. Wang, and D.-H. Lee, Phys. Rev. B **86**, 134508 (2012).
[62]R. H. Liu, T. Wu, G. Wu, H. Chen, X. F. Wang, Y. L. Xie, J. J. Ying, Y. J. Yan, Q. J. Li, B. C. Shi, W. S. Chu, Z. Y. Wu, and X. H. Chen, Nature (London) **459**, 64 (2009).
[63]A. Lanzara, P. V. Bogdanov, X. J. Zhou, S. A. Kellar, D. L. Feng, E. D. Lu, T. Yoshida, H. Eisaki, A. Fujimori, K. Kishio, J.-I. Shimoyama, T. Noda, S. Uchida, Z. Hussain, and Z.-X. Shen, Nature (London) **412**, 510 (2001).
[64]T. Yildirim, Phys. Rev. Lett. **102**, 037003 (2009).
[65]F. Yndurain and J. M. Soler, Phys. Rev. B **79**, 134506 (2009).
[66]F. Yndurain, Europhys. Lett. **94**, 37001 (2011).
[67]I. I. Mazin, D. J. Singh, M. D. Johannes, and M. H. Du, Phys. Rev. Lett. **101**, 057003 (2008).
[68]T. Yildirim, Phys. Rev. Lett. **101**, 057010 (2008).
[69]Q. Si and E. Abrahams, Phys. Rev. Lett. **101**, 076401 (2008).
[70]F. J. Ma, Z. Y. Lu, and T. Xiang, Phys. Rev. B **78**, 224517 (2008).

[71] J. Zhao, D. X. Yao, S. Li, T. Hong, Y. Chen, S. Chang, W. Ratcliff, J. W. Lynn, H. A. Mook, G. F. Chen, J. L. Luo, N. L. Wang, E. W. Carlson, J. Hu, and P. Dai, Phys. Rev. Lett. **101**, 167203 (2008).

[72] J. Zhao, D. T. Adroja, D. X. Yao, R. Bewley, S. Li, X. F. Wang, G. Wu, X. H. Chen, J. P. Hu, and P. C. Dai, Nat. Phys. **5**, 555 (2009).

[73] A. Kokalj, Comput. Mater. Sci. **28**, 155 (2003). Code available from http://www.xcrysden.org.